

## Article

# The Study of Metal Corrosion Resistance near Weld Joints When Erecting Building and Structures Composed of Precast Structures

Pyotr V. Zgonnik \*, Alyona A. Kuzhaeva and Igor V. Berlinskiy

Faculty of Mineral Raw Material Processing, Saint-Petersburg Mining University, 21st Line, 2, 199106 Saint Petersburg, Russia; kaarlo@mail.ru (A.A.K.); bgarris@yandex.ru (I.V.B.)

\* Correspondence: piter\_cat@mail.ru or zgonnik@spmi.ru

**Abstract:** Corrosion processes of the most common steel grades in various environments are the subject of numerous studies. At the same time, the corrosion of welded joints hidden in concrete thickness has not yet been studied. The authors set themselves the task of investigating this process. For this purpose, the corrosion resistance of several metals (grade St.3, U7 and their weld joints) was studied in standard test solutions, simulating a concrete pore liquid, containing sodium carbonates and hydrocarbonates, and sodium chlorides. Data on comparative corrosion resistance in saline media for specified materials were obtained. It was shown that the corrosion rate depends on the ease of CO<sub>2</sub> ingress into the solution, and, to a lesser degree, on the metal microstructure. The surface character of the metal samples and the composition of corrosion products were investigated by scanning electron microscopy and an X-ray diffraction analysis. Chemical forms of surface compounds were determined. For the first time, it is clearly shown that the electrode coating flowing during welding does not always protect the weld from corrosion, as was previously believed. The corrosion rate, in this case, is just the same as at the surface of the metal plate of a similar composition. In the conclusion of this work, it is emphasized that in the case of alkaline and chloride-containing media, the protective coating falling from the electrode to the weld does not protect it sufficiently from corrosion.

**Keywords:** corrosion resistance; welding unit; concrete; concrete pore liquid; carbon dioxide; scanning electron microscopy; X-ray diffraction analysis; gravimetry; weight loss kinetics; surface defects



**Citation:** Zgonnik, P.V.; Kuzhaeva, A.A.; Berlinskiy, I.V. The Study of Metal Corrosion Resistance near Weld Joints When Erecting Building and Structures Composed of Precast Structures. *Appl. Sci.* **2022**, *12*, 2518. <https://doi.org/10.3390/app12052518>

Academic Editors: Olga Smirnova and Grigoriy Yakovlev

Received: 30 November 2021

Accepted: 22 February 2022

Published: 28 February 2022

**Publisher's Note:** MDPI stays neutral with regard to jurisdictional claims in published maps and institutional affiliations.



**Copyright:** © 2022 by the authors. Licensee MDPI, Basel, Switzerland. This article is an open access article distributed under the terms and conditions of the Creative Commons Attribution (CC BY) license (<https://creativecommons.org/licenses/by/4.0/>).

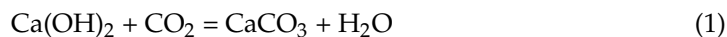
## 1. Introduction

Corrosion is under the continuous scrutiny of researchers [1,2]. By average estimates, currently, direct losses of metal from corrosion are approx. 4–5 percent of the national income of industrially developed countries, and not less than 10 percent of smelted metal, that is, 20 million tons per year. Practical engineers undertake maximum necessary measures for the corrosion protection of process equipment and engineering structures [3–6]. Article [3] examines the corrosion of underground pipelines and suggests new ways to protect against it. In work [4], the effect of shear stress on the wall of technological pipelines on the intensity of carbon dioxide corrosion is studied. Articles [5,6] discuss the chemical and thermal treatment of steel in low-melting solutions. The authors of article [7] compare the data on corrosion in different continental regions on Earth. Paper [8] is devoted to the repair of a precast reinforced concrete residential building. This article contains important information concerning the corrosion processes of steel reinforcement inside reinforced concrete. Monograph [9] contains extensive material, devoted also to the corrosion of steel reinforcement. Authors of monograph [9] summarize materials on this topic. Monograph [10] is devoted to concrete corrosion and contains numerous examples of concrete decomposition in seawater. The interrelation of concrete and reinforcement destruction is considered on numerous examples. Paper [11] is listed as a good illustration of this type of investigation.

Currently, research is continuing in the field of corrosion of bimetallic metal compounds, a good example of which are the works [12,13]. A number of works are related to the general problems of assessing the mechanical strength of materials, including those of welds [14,15] and practical methods of control [16,17]. The modern technique of corrosion control is also discussed in papers [18,19]. Various mathematical models, in particular the graph theory, have been used to describe the corrosion process [20]. Paper [21] deals with the corrosion protection of steel pipes in petrochemical production. Maksarov et al. paid much attention to improving the quality of the further processing of welded products [22–25]. Paper [26] is devoted to corrosion investigations in the atmosphere.

Currently, conducted research mostly affects the phenomena of atmospheric corrosion, a good example of this is the extensive and scrupulous work in [7]. As experience in the operation of precast concrete buildings shows, over time, various difficult-to-remove defects occur in concrete, which cause the corrosion of the reinforcement [8]. The problem of corrosion is substantive, where one or another fabricated metal part that is inaccessible for visual and instrument inspection corrodes. In particular, this applies to the assembly process of buildings and structures of precast concrete. The total output of fabricating yards is under production regulations and under the strict control of factory laboratories. In the overwhelming majority of cases, the fabricating yards produce products by autoclaving, during which the concrete setting occurs under an elevated temperature (191 °C) and pressure, exceeding the atmosphere's pressure by 10% [9]. However, the assembly occurs outdoors, whereby a strict quality control of joint sealing between the mating structures, or cement grout or concrete drying temperature is impossible [10,11]. These determine the comparatively inferior quality of concrete quality in joints. To join two precast structure elements, electric welding is generally used. The characteristic feature of electric welding is fast metal heating and cooling, resulting in the formation of micro-cracks near the weld joint. Quite often, such heating is performed repeatedly. Moreover, when welding, a change in the mating metals' microstructure near the weld occurs [12,13]. All the above-mentioned factors can increase the metal corrosion. Currently, effective methods of quality control of welding joints [13–23] as well as the remote monitoring of the operational characteristics of structures have already been developed. Recently, intensive research has also been conducted aimed at the early detection of corrosion [18,19]. However, when assembling elements from reinforced concrete, it is practically impossible to monitor the corrosion near the weld joint after sealing the joint between the concrete goods by cement grout [9].

It is known that concrete pore liquid has a pH of approx. 12, which stipulates reinforcing steel passivation and prevents its corrosion in the bulk of concrete. During the operation, moisture and CO<sub>2</sub> diffuse inside concrete, with strongly alkaline solutions of concrete pore liquid (with pH ≈ 11.3–12.5) reacting with CO<sub>2</sub> with the calcium carbonate generation [9]:



The further development of the process results in hydrocarbonate formation, shifting the pH value towards neutral solutions, reaching a pH of 9, which results in the depassivation of the protective oxide coating on the metal, creating favorable conditions for corrosion. It is known that iron corrosion is the most intense, in the pH range from 4 to 10 [27,28]



Reinforcement corrosion results in the formation of a loose mass of hydrated ferric oxides, the volume of which exceeds the volume of the initial metal-reinforcing element. This, in turn, results in the mechanical failure of concrete [29].

A large body of research is devoted to concrete corrosion [30] (a review is given in paper [27]) and corrosion in saturated lime solutions [31]; however, it does not concern the peculiarities of the corrosion of weld joints and joining the reinforcement when assembling concrete goods. The aim of this paper is to study the metal corrosion near the weld joint in the standard test medium with a pH close to the pH of a solution in the concrete pores.

## 2. Materials

A list of studied structural materials and their composition is given in Table 1. Distilled water, sodium chloride (chemically pure), sodium carbonate  $\text{Na}_2\text{CO}_3 \times 10\text{H}_2\text{O}$  (pure) and sodium hydrocarbonate (chemically pure) were used to prepare the saline solutions. Saline media composition is listed in Table 2.

**Table 1.** Composition of the studied structural materials.

Control Parameters	Material Grade		
	U7	St.3	ANO-4
Components	GOST 1435–99	GOST 380–2005	GOST 5.1215–72
As	-	up to 0.08	-
C	0.66–0.73	0.14–0.22	up to 0.10
Cr	up to 0.2	up to 0.3	-
Cu	up to 0.25	up to 0.3	-
Fe	base	base	base
Mn	0.17–0.33	0.4–0.65	0.6–0.8
Ni	up to 0.25	up to 0.3	-
N	-	up to 0.008	-
P	up to 0.03	up to 0.04	up to 0.035
S	up to 0.028	up to 0.05	up to 0.035
Si	0.17–0.33	0.05–0.17	up to 0.18

**Table 2.** Summary data on the study of structural materials corrosion resistance.

Sample No.	Sample Material	Saline Media Composition, wt. %			Initial Corrosion Rate Per First Day, $\text{g}/\text{cm}^3 \text{ Day} \cdot 10^4$
		$\text{Na}_2\text{CO}_3$	$\text{NaHCO}_3$	$\text{NaCl}$	
1	St3	4.2	33.6	3.5	3.4
		4.2	33.6	-	1.8
2	U7	4.2	33.6	3.5	1.2
		4.2	33.6	-	0.95
3	Weld joint St3-St3	4.2	33.6	3.5	3.2
		4.2	33.6	-	2.13
4	Weld joint St3-U7	4.2	33.6	3.5	3.42
		4.2	33.6	-	2.4
5	Weld joint U7-U7	4.2	33.6	3.5	3.3
		4.2	33.6	-	2.10

## 3. Methods

The study of structural materials corrosion in solutions was carried out in both static conditions and with agitation. In the experiments with agitation, a periodical agitation of the solution was carried out once a day for 1 h by a submerged mixing device at the rate of  $\approx 600$  RPM. The technique of the experiment with agitation is described in detail in our previous works [32,33]. The sheet metal samples were welded by ANO-4 electrodes 2 mm<sup>2</sup> in diameter with a welding current of 40 A. Then, the surface was mechanically cleaned and the 10 cm<sup>2</sup> plates were cut out. The obtained 10 cm<sup>2</sup> plates were placed into the solution (Table 2) and exposed for 1–62 days. The pH of the model solution was about 11.2–11.5 and changed slightly over time. At the same time, two parallel experimental series were performed in dynamic mode and three in static mode. Corrosion rate monitoring was

implemented by weighting by the use of the analytical balance VLO-200 (Russia). The reaction rate was determined by the loss in weight of the plate for the specified time period:

$$v = \frac{\Delta m}{S \cdot \Delta \tau} \quad (3)$$

where:

$v$ —corrosion rate;

$\Delta m$ —sample mass variation;

$S$ —sample area;

$\tau$ —exposure time.

The concentration of iron in the solution was determined via the spectrophotometric method [29]. Spectrophotometric determination of iron (III) in solution was carried out by the use of strongly colored complexes with thiocyanate ions. Photometric analysis was performed on the KFK-3 instrument (Russia) at a wavelength of 480 nm (when the maximum absorption of the thiocyanate ion was observed). Photometry was carried out according to a two-beam scheme using a comparison solution with a cuvette length of 2 cm. Quantitative determination was performed using a pre-constructed calibration dependence with standard solutions. This method is very sensitive and allows to confidently determine the concentrations of iron (III) ions up to  $10^{-5}$  mol/L.

As the obtained data show (Table 2), the samples with a weld joint turned out to be more apt to corrosion than the initial allow samples. As expected, steel grade St3 showed lesser resistance to corrosion compared to U7, which was clearly seen by the corrosion rate (Table 2). Among weld joints, the joint of two steel grade St3 plates showed higher resistance to corrosion. The main cause of the observed feature was probably defects in the structure of the metal resulting from thermal shock accompanying electric arc welding.

The chemical and phase composition of the surface compounds formed during corrosion was studied by X-ray diffraction phase analysis.

The measurements were carried out using a powder X-ray diffractometer D2 Phaser (Bruker, Germany) using CoK $\alpha$  radiation. XRD quantitative analyses were performed by full-profile pattern refinement (Rietveld method) with Topas 5.0 software. A good fit was obtained for each of the samples without introducing amorphous phases into the models even though the overlapping wide (due to small crystallite size and microstrain) reflections might have produced an impression on partial amorphization.

The elemental composition of the surface was determined using energy-dispersive X-ray microanalysis. The microrelief of the surface was studied using scanning electron microscopy.

Electron microscopic studies were performed on a scanning electron microscope Supra 55 VP by Carl Zeiss (Germany). The samples used for electron microscopic examination were coated with platinum on the Q150T high-vacuum deposition unit of Quorum Technologies (Great Britain). Energy-dispersive X-ray microanalysis was performed on the console EDX 80 firm Oxford Instruments Nano Analysis (UK) to the scanning electron microscope (Supra 55 VP, Carl Zeiss (Germany)).

#### 4. Results and Discussion

As shown in Figure 1, agitation contributed substantially to the corrosion mechanism. With static exposure in the standard test solution (curve 1), the reaction occurred under the diffusion control and, with a surface layer saturation near the metal, the process retardation took place.

As we could expect, the decrease in the corrosion rate during the first 20 days was apparently due to the gradual shielding of the metal surface with hydrated oxides and other corrosion products. The agitation probably removed the diffusion limitations on the reaction rate [30,31]. We assume that the increase in the corrosion rate after 40 days was due to kinetic features. With every subsequent agitation, the saline solution saturation by oxygen and CO $_2$  up to the constant values of concentration occurred. A similar nature of

relationship between the corrosion rate and the exposure time for the sample with a weld joint (Figure 2) showed that the metal microrelief and the likely standard electric potential difference of two different alloys were also not the reason of the observed peculiarity.

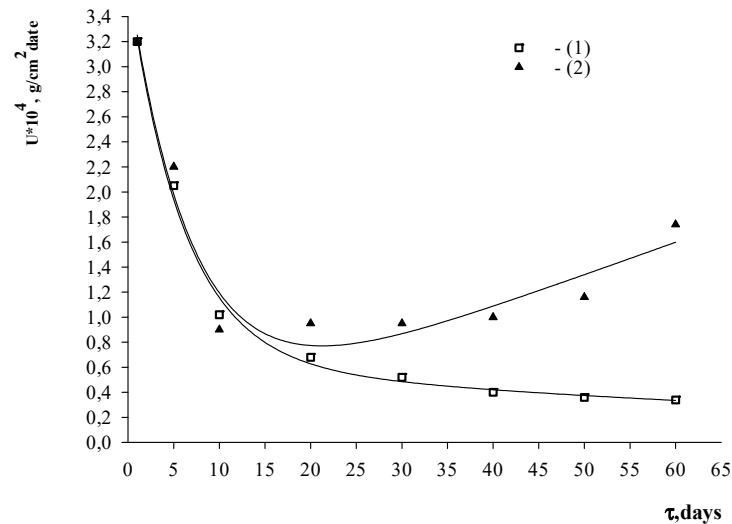


**Figure 1.** Variation of St3 (sample No. 1) corrosion rate in the solution containing NaCl. 1—in static conditions; 2—with agitation.

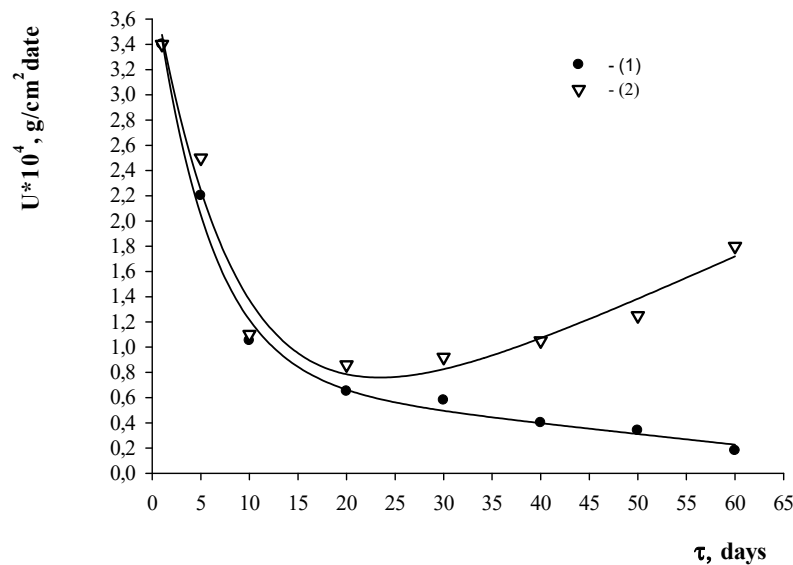


**Figure 2.** Variation of the corrosion rate of the plate with a weld joint (sample No. 4) in the solution containing NaCl. 1—in static conditions; 2—with agitation.

The above-mentioned factors impacted the overall dissolution rate, but this impact was invariable in time. One could cautiously surmise that, in this case, there were kinetic difficulties caused by the occurrence of the following reaction:



With that, metal surface passivation by the deposition of formed calcium carbonate would be likely to occur. It would gradually cease as the standard test solution would absorb  $\text{CO}_2$  from the air in the quantities, sufficient for the reaction described by Equation (2).

Another possible reason for the abrupt change in the reaction rate during intermittent agitation after 20 days was the development of porosity on the sample surface as the metal was oxidized. Within the framework of these concepts, it was easy to explain the

significant difference in the dynamics of the corrosion rate changes over time for cases with intermittent stirring and without it. It was agitation that helped saturate the pores with “fresh” portions of the solution. Existing porometry methods require surface dewatering. Unfortunately, drying the sample caused very significant changes in the chemical structure of hydrated oxides on the metal surface. The complete dehydration of surface compounds inevitably leads not only to a change in the size of the pores, but also to a complete change in the relief of the surface. These circumstances caused it to be impracticable to correctly take into account changes in the porous structure of the corrosion products in the solution environment. Due to these reasons, it was also not possible to provide an adequate mathematical interpretation of the diffusion in the case under consideration.

It cannot be ruled out that the noted peculiarity of the process with periodic agitation was associated with the transition of the iron ion to the solution and its further completion of oxidation. However, the data on the iron content in the solution (Figures 3 and 4) prevented us from stating this with confidence.

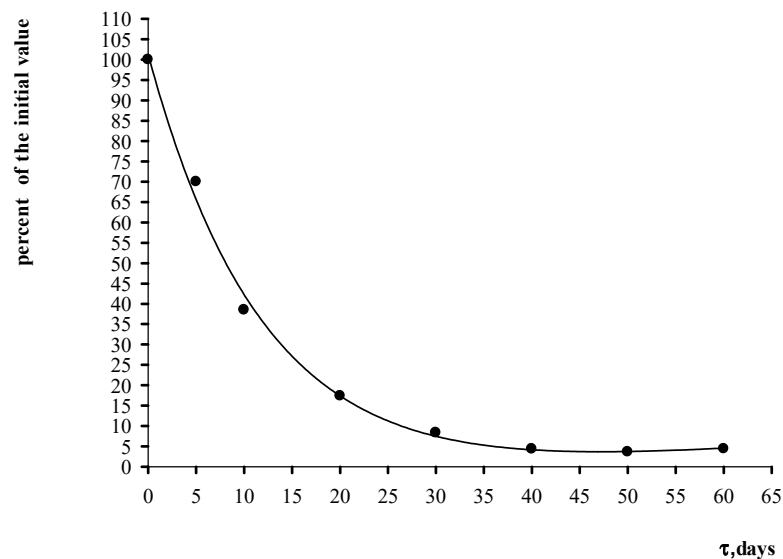


**Figure 3.** The history of steel grade St3 (sample No. 1) corrosion rate in the NaCl-containing solution, determined by iron availability in the saline solution without agitation.

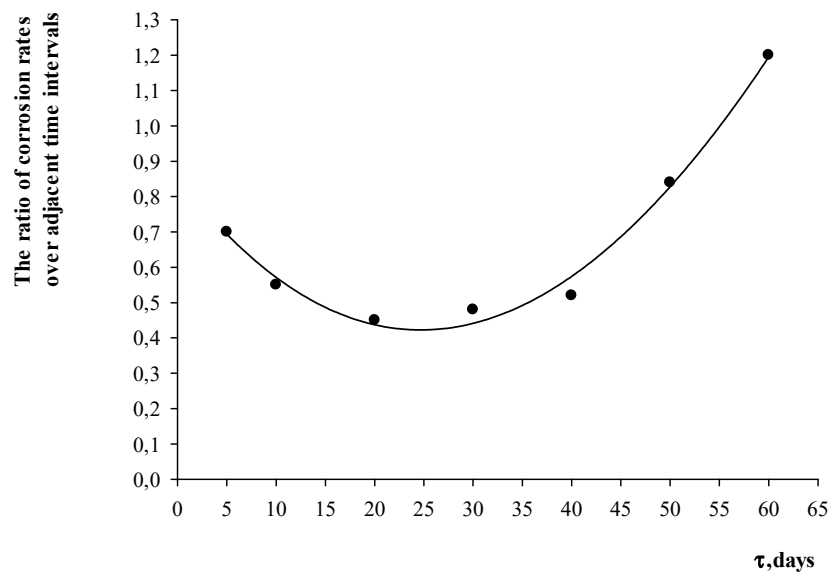


**Figure 4.** The history of steel grade St3 (sample No. 1) corrosion rate in the NaCl-containing solution, determined by iron availability in the saline solution with agitation.

Incidentally, it is known that iron oxides have a nonstoichiometric structure, and the degree of corrosion in time depends on the residual porosity (capillarity) of FeO [34]. Until recently, new information has been published on the effect of FeCO<sub>3</sub> on the process of iron corrosion [35,36].

The typical results of the elemental analysis of the surface layer are presented in Table 3. As follows from the data in Table 3, the main surface compounds are iron (III) oxides. The relatively high carbon content is probably due to the presence of carbonates.

**Table 3.** Summary data on the study of the elemental composition of the samples welded between steel St3 and steel U7 surface after exposure for 60 days, according to energy-dispersive X-ray microanalysis.

Spectrum No	B Stat.	Contents at the Surface of the Sample Material, wt. %						Total
		C	O	Na	S	Cl	Fe	
1	Y	6.95	34.19	0.14	0.49	0.31	57.93	100.00
2	Y	8.14	31.65	0.13	0.56	0.27	59.24	100.00
3	Y	7.44	35.01	0.00	0.50	0.31	56.74	100.00
4	Y	8.62	34.13	0.20	0.46	0.27	56.32	100.00
5	Y	5.15	32.87	0.21	0.98	0.47	60.32	100.00
6	Y	5.44	34.00	0.15	0.86	0.25	59.30	100.00
7	Y	5.15	33.58	0.08	0.30	0.26	60.63	100.00
8	Y	7.74	31.19	0.13	0.36	0.22	60.36	100.00
9	Y	7.43	31.63	0.15	0.37	0.22	60.21	100.00
10	Y	6.04	31.06	0.15	0.70	0.41	61.65	100.00
Average		6.81	32.93	0.13	0.56	0.30	59.27	100.00
Standard deviation		1.28	1.44	0.06	0.22	0.08	1.75	
max.		8.62	35.01	0.21	0.98	0.47	61.65	
min.		5.15	31.06	0.00	0.30	0.22	56.32	

An electron microscopic study of the surface of the samples after 60 days of exposition indicated the presence of a loose disordered structure on their surface with different crystallite sizes (Figures 5–8). In the micrographs, one could observe spherulites of calcium carbonate, lineal structures of iron (III) compounds (also see Table 4) and (in the case of a weld joint) hollows associated with gas emission presumably in the process of electric arc welding. There were, however, certain differences in the structure of the surface layer in the case of samples of St3, U7 and, in particular, welded joints.

The phase composition of the rust of the samples under investigation after 60 days exposition is presented in Table 4. As can be seen, the corrosion products of St3, U7 and the weld contained, in general, oxides–hydroxides, and some qualitative and quantitative differences were related to the composition of the starting metals. The presence of albite and, probably, the traces of muscovite was due to the coating of the welding electrode. The quantitative definitions should not be considered too accurate, because the main phases were poorly crystallized. As for the crystallinity of the defective phases, it could be expected that it was their defectiveness (oxygen deficiency, vacancies, stresses, etc.) that prevented the formation of large crystals. As it was shown above (Table 2), the presence of these components did not have a decisive effect on the corrosion process. Typical diffractograms are shown at Figures 9–11.

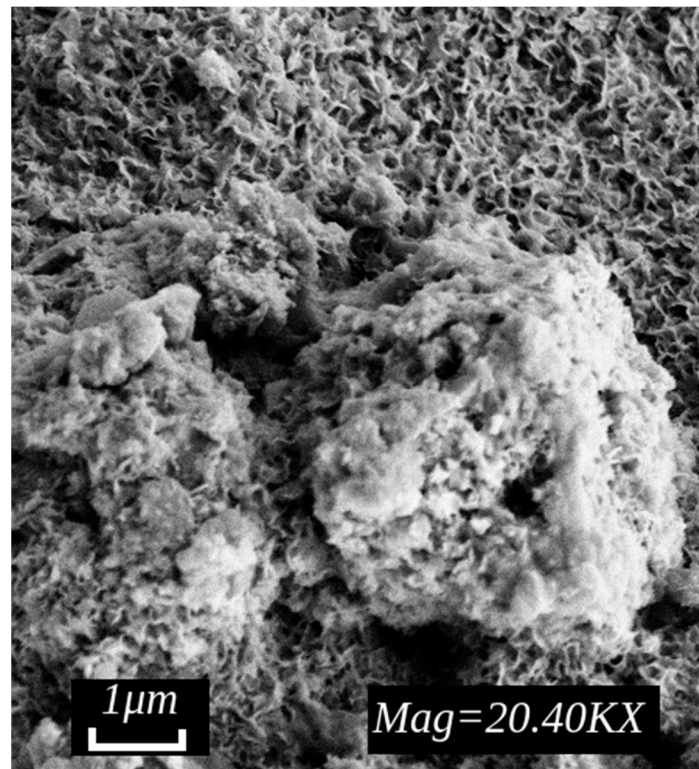


**Figure 5.** Electronic microphotograph of the steel St3 surface after 60 days of exposure. Linear structure— $\text{FeO}(\text{OH})$ ; bulk structure— $\text{CaCO}_3$  and its co-crystallized components.

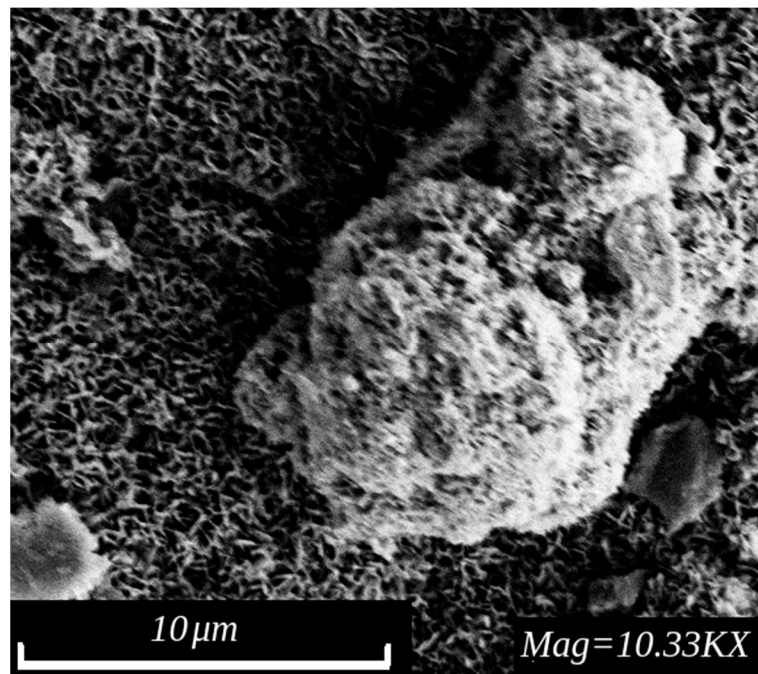


**Figure 6.** Electronic microphotograph of the steel St3 surface after 60 days of exposure. Linear structure— $\text{FeO}(\text{OH})$ ; bulk structure— $\text{CaCO}_3$  and its co-crystallized components.

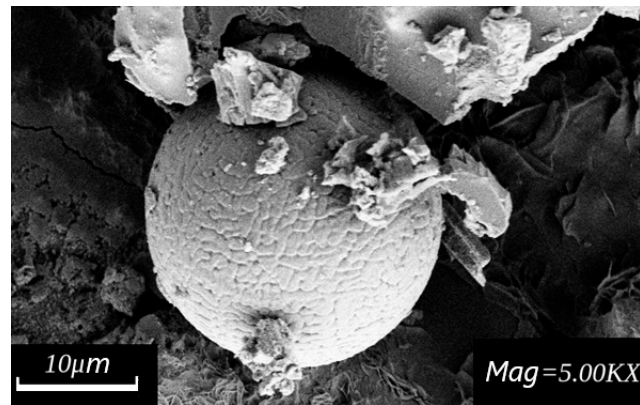


**Figure 7.** Electronic microphotograph of the weld between steel St3 and steel U7 (surface after 60 days of exposure). “Wasp’s nest” structure is calcium carbonate spherulite and angular plate structure is FeO(OH).

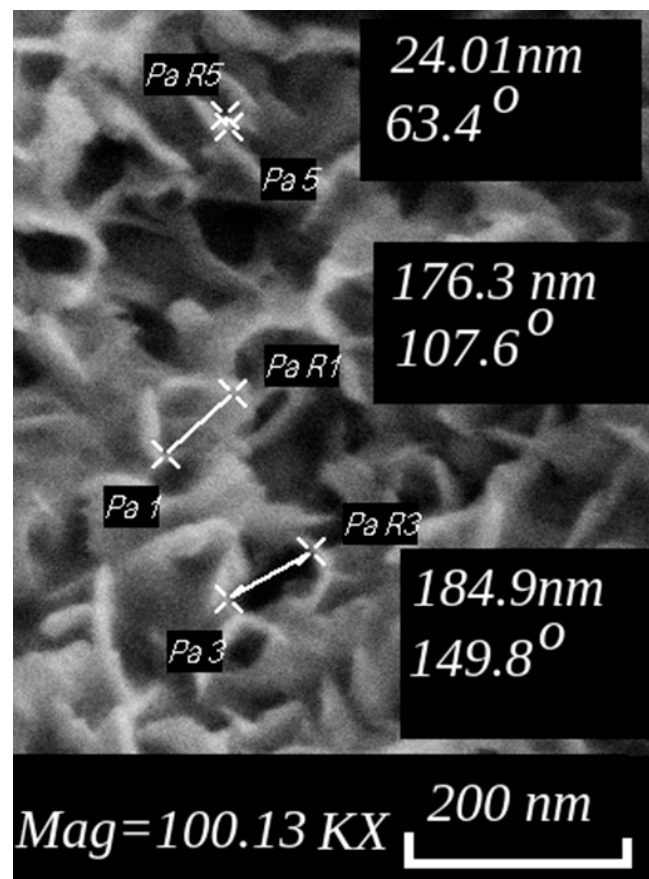


**Figure 8.** Electronic microphotograph of the surface of steel St3 surface after 60 days exposure with structural elements measurement.

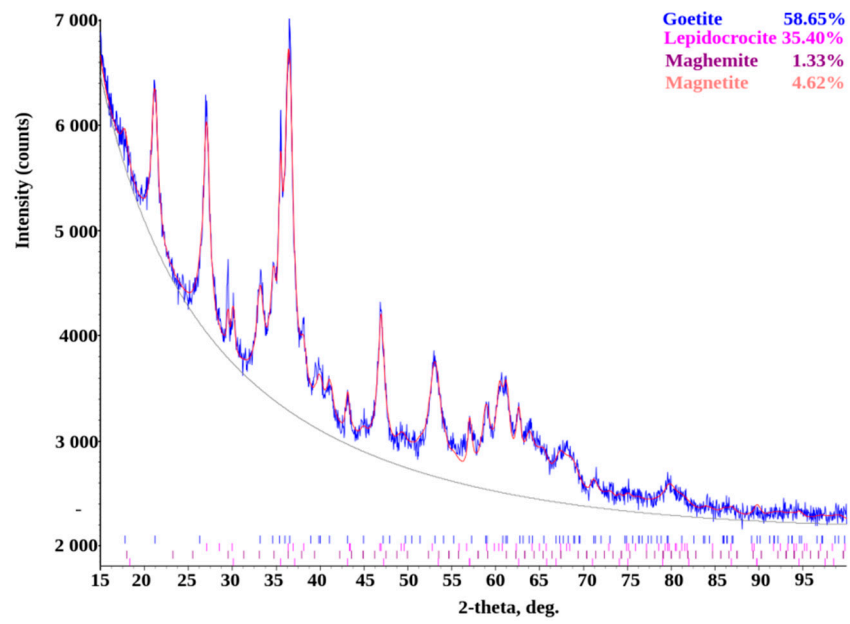


**Figure 9.** Diffractogram of the St3 surface compounds. Vertical bars at the bottom of the graph mark the peak positions of the identified phases.

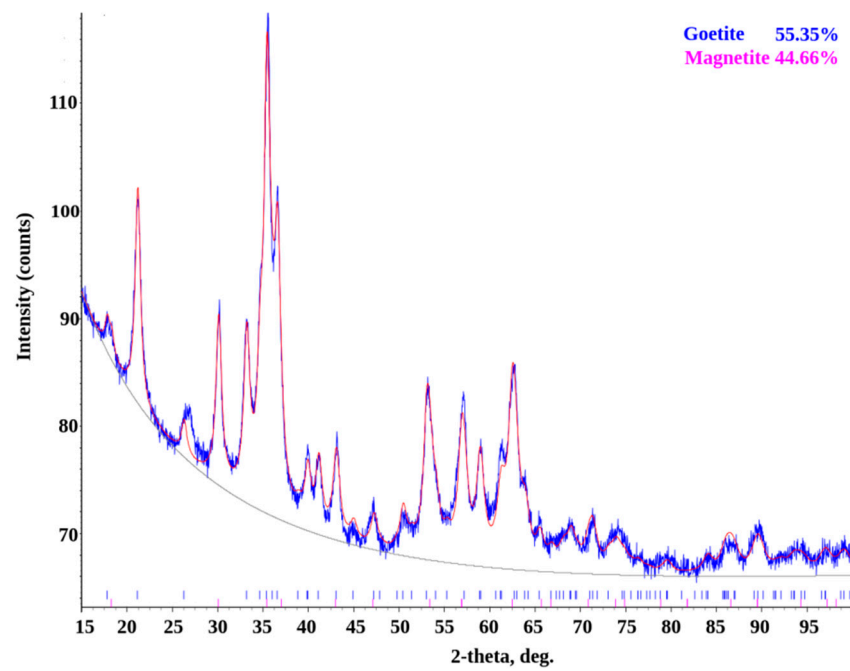


**Figure 10.** Diffractogram of the of the U7 surface compounds. Vertical bars at the bottom of the graph mark the peak positions of the identified phases.

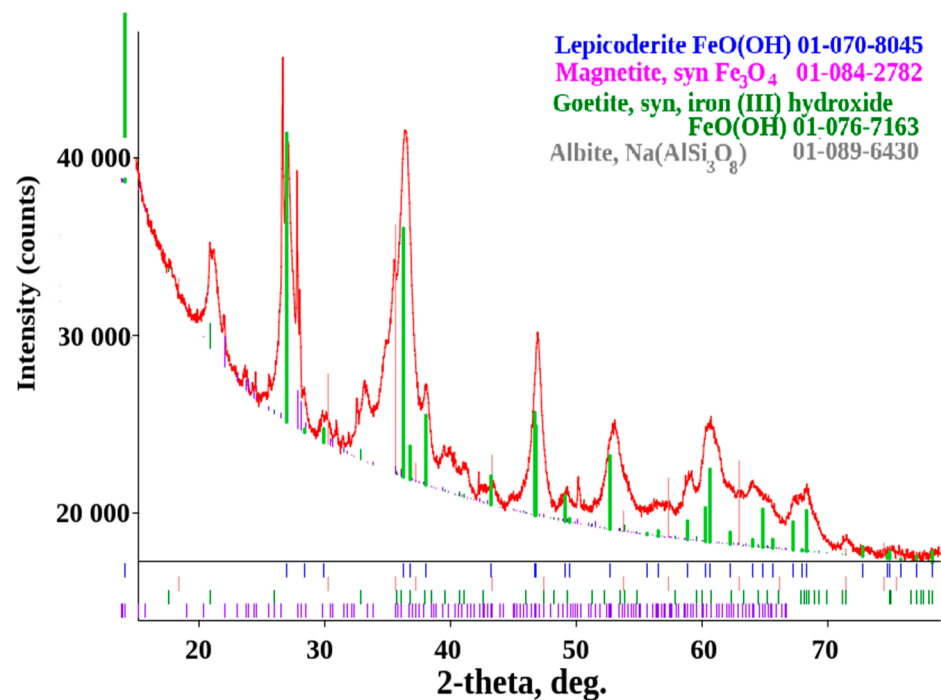


**Figure 11.** Diffractogram of the weld joint St3-U7 surface compounds. Vertical bars at the bottom of the graph mark the peak positions of the identified phases.

**Table 4.** Summary data on the study of the phase composition of samples after exposure for 60 days according to the X-ray phase study.

No	Phase Name	Formula	Contains at the Surface of the Sample Material, %		
			St3	U7	Weld Joint St3-U7
1	Iron(III) oxide hydroxide, goethite	FeO(OH)	58.65	55.35	44.51
2	Lepidocrocite	FeO(OH)	35.40	-	38.29
4	Magnetite	Fe <sub>3</sub> O <sub>4</sub>	4.62	44.65	4.16
5	Maghemite	Fe <sub>3</sub> O <sub>4</sub>	1.33	-	-
6	Albite	Na[AlSi <sub>3</sub> O <sub>8</sub> ]	-	-	13.03
7	Muscovite	KAl <sub>2</sub> [AlSi <sub>3</sub> O <sub>10</sub> ](OH) <sub>2</sub>	-	-	traces

## 5. Conclusions

In this work, it was shown that the corrosion process in model alkaline and alkaline-chloride media proceeded by a complex mechanism. The predominance of kinetic or diffusion control was traditionally determined by the presence or absence of agitation. However, this was probably not the only factor. The rate of the corrosion process was also affected by the surface relief, the specifics of the existence of surface phases of variable composition as well as the conditions of the equilibrium existence of surface compounds. The situation was complicated by the fact that the direct porometric analysis of the surface under these research conditions was associated with significant difficulties, even if it was still possible.

For a long time, it was assumed that the electrode coating melted during electric welding, flowed down to the metal surface and protected the weld from corrosion. However, as follows from our results, this useful phenomenon was not typical for all cases. In

particular, this applied to alkaline and (or) chloride-containing media. One of the solutions to the problem is to provide a better corrosion protection of reinforcement splicing for concrete goods, and the quality of a concrete seal for block joints should be improved. In specific cases, additional insulating materials on metals should be applied as offered in paper [37]. It is necessary, however, to take into account the fact that hydrophobic coatings weakened the adhesion of concrete to metal. This work was just the beginning of the study of the corrosion of welds in the thickness of concrete. We expect to continue these studies further. Currently, concretes based on multicomponent binders are being developed and used [38,39], which can lead to a change in the pH of the liquid phase in the concrete structure and, accordingly, affect the corrosion of welded joints in the reinforcement [40]. This requires further advanced research of the corrosion processes of welded joints in the concrete thickness.

**Author Contributions:** Conceptualization, P.V.Z. and A.A.K.; methodology, P.V.Z.; validation, P.V.Z. and A.A.K.; formal analysis, P.V.Z.; investigation, P.V.Z. and A.A.K., graphical distribution, I.V.B. and P.V.Z.; writing—original draft preparation, P.V.Z.; writing—review and editing, P.V.Z. and A.A.K.; visualization, I.V.B.; supervision, P.V.Z. and A.A.K.; project administration, A.A.K.; funding acquisition—centrally through the University’s distribution system. All authors have read and agreed to the published version of the manuscript.

**Funding:** This research was carried out at the expense of a subsidy for the implementation of the state task in the field of scientific activity for 2021, No. FSRW-2020-0014 (Russia).

**Data Availability Statement:** All the data given in this article are the results of the original research conducted by the authors and are not drawn from the general public databases or archives.

**Acknowledgments:** The authors express their gratitude to Associate Professor Ivan I. Ivanov, a former employee of the Department of General Chemistry of St.-Petersburg Mining University for participating in the discussion of the work and valuable advice. The authors are also grateful to Associate Igor A. Kasatkin from the St.-Petersburg State University Resource Center “X-Ray Diffraction Research Methods” for advice on interpreting the results.

**Conflicts of Interest:** The authors declare no conflict of interests.

## References

1. Balasubramaniam, R. On the corrosion resistance of the Delhi iron pillar. *Corros. Sci.* **2000**, *42*, 2103–2129. [[CrossRef](#)]
2. Dwivedi, D.; Mata, J.P.; Salvemini, F.; Rowles, M.R.; Becker, T.; Lepková, K. Uncovering the superior corrosion resistance of iron made via ancient Indian iron-making practice. *Sci. Rep.* **2021**, *11*, 4221. [[CrossRef](#)] [[PubMed](#)]
3. Goldobina, L.A.; Orlov, P.S. Analysis of the corrosion destruction causes in underground pipelines and new solutions for increasing corrosion steel’s resistance. *J. Min. Inst.* **2016**, *219*, 459. [[CrossRef](#)]
4. Ponomarev, A.I.; Yusupov, A.D. Effect of shear stress on the wall of technological pipelines at a gas condensate field on the intensity of carbon dioxide corrosion. *J. Min. Inst.* **2020**, *244*, 439–447. [[CrossRef](#)]
5. Sivenkov, A.V. Chemical-thermal treatment of steel in an environment of low-melting solutions. *J. Min. Inst.* **2014**, *209*, 244–249.
6. Dzhabbarov, S.N.; Pryakhin, E.I. Using the Diffusion Saturation Technology for the Surface of Different Steel Products from Melts of Low-Melting Metals. *Key Eng. Mater.* **2020**, *836*, 36–40. [[CrossRef](#)]
7. Panchenko, Y.M.; Marshakov, A.I.; Nikolaeva, L.A.; Igonin, T.N. Estimating the First-year Corrosion Losses of Structural Metals for Continental Regions of the World. *Siv. Eng. J.* **2020**, *6*, 1503–1518. [[CrossRef](#)]
8. Shannag, M.J.; Higazey, M. Strengthening and Repair of a Precast Reinforced Concrete Residential Building. *Civ. Eng. J.* **2020**, *12*, 2457–2473. [[CrossRef](#)]
9. Dvorkin, L.I. (Ed.) Betonovedenie (Concrete study). Monograph. In *Osnovnye Raznovidnosti Betonov (Major Concrete Varieties); Infra-Inzheneriya Publ.: Vologda, Russia, 2021; Volume 2*, pp. 152–608. (In Russian)
10. Moskvina, V.M.; Ivanov, F.M.; Alekseev, S.N.; Guzeev, E.A. *Korroziya Betona i Zhelezobetona, Metody Ikh Zashchity (Corrosion of Concrete and Reinforced Concrete, the Methods of Their Protection); Stroyizdat Publ.: Moscow, Russia, 1980; pp. 533–536.* (In Russian)
11. Belentsov, Y.A.; Smirnova, O.M.; Kazanskaya, L.F. Improvement of competitive edge of precast reinforced concrete by increasing the reliability level and quality control. *IOP Conf. Ser. Mater. Sci. Eng.* **2019**, *666*, 012037. [[CrossRef](#)]
12. Piskarev, P.Y.; Gervash, A.A.; Vologzhanina, S.A.; Ermakov, B.S.; Kudryavceva, A.M. Study of the Bimetallic Joint CuCrZr/316L(N). *Mater. Sci. Forum* **2021**, *1040*, 8–14. [[CrossRef](#)]
13. Sharapova, D.M.; Sharapov, M.G.; Sharonov, N.I. Structure Formation of Butt Joints Made of Aluminum Alloys to Ensure the Quality of Mechanical Engineering Products. *Mater. Sci. Forum* **2021**, *1022*, 119–126. [[CrossRef](#)]

14. Nosov, V.V.; Grigoriev, E.V.; Peretyatko, S.A.; Artyushchenko, A.P. Nanotechnologies of Strength Control of Materials. *Mater. Sci. Forum* **2021**, *1040*, 101–108. [[CrossRef](#)]
15. Nosov, V.V.; Zelenskii, N.A. Estimating the strength of welded hull elements of a submersible based on the micromechanical model of temporal dependences of acoustic-emission parameters. *Mater. Sci. Forum* **2017**, *53*, 89–95. [[CrossRef](#)]
16. Nosov, V.V. On the principles of optimizing the technologies of acoustic-emission strength control of industrial objects. *Mater. Sci. Forum Russ.* **2016**, *52*, 386–399. [[CrossRef](#)]
17. Pecherskaya, E.A.; Golubkov, P.E.; Artamonov, D.V.; Pecherskiy, A.V.; Mel'Nikov, O.A.; Shepeleva, A.E. The Model of the Relationship of the of Micro-arc Oxidation Process Parameters Based on Graph Theory. In *Moscow Workshop on Electronic and Networking Technologies (MWENT-2020)*; Publishing House of the National Research University Higher School of Economics: Moscow, Russia, 2020. [[CrossRef](#)]
18. Liu, Z.; Jia, R.; Chen, F.; Yan, G.; Tian, W.; Zhang, J.; Zhang, J. Electrochemical process of early-stage corrosion detection based on N-doped carbon dots with superior Fe<sup>3+</sup> responsiveness. *J. Colloid Interface Sci.* **2021**, *606 Pt 1*, 567–576. [[CrossRef](#)] [[PubMed](#)]
19. Potapov, I.A.; Kondrat'ev, A.V. Remote monitoring of pipelines using tele communications technology. *J. Min. Inst.* **2014**, *209*, 138–143.
20. Issa, B.; Bazhin, V.Y.; Telyakov, N.M.; Telyakov, A. Increasing of corrosion resistance of welded radiant and convection coiled-pipes in tubular furnaces at kinef crude oil refinery, Technical Sessions Proceedings. In Proceedings of the 6th Youth Forum of the World Petroleum Council—Future Leaders Forum, Saint Petersburg, Russia, 23–28 June 2019; pp. 243–249. [[CrossRef](#)]
21. Syzrantseva, K.V.; Syzrantsev, V.N.; Dvoynikov, M.V. The application of finite element analysis during development of the Integral Strain Gauges calibration method for the study of the welded construction. *Mater. Sci. Forum* **2017**, *177*, 12133. [[CrossRef](#)]
22. Maksarov, V.V.; Vasin, S.A.; Efimov, A.E. Dynamic Stabilization in Reaming Internal Surfaces of Welded Components. *Russ. Eng. Res.* **2021**, *41*, 939–943. [[CrossRef](#)]
23. Maksarov, V.V.; Efimov, A.E.; Olt, J.J. Improving the quality of hole processing in welded products made of dissimilar materials with a new boring tool. *Int. J. Adv. Manuf. Technol.* **2021**, *118*, 1027–1042. [[CrossRef](#)]
24. Maksarov, V.; Khalimonenko, A.; Olt, J. Managing the process of machining on machines on the basis of dynamic modelling for a technological system. *J. Silic. Based Compos. Mater.* **2017**, *69*, 66–71. [[CrossRef](#)]
25. Maksarov, V.V.; Vasin, S.A.; Efimov, A.E.; Keksin, A.I. Influence of the Microstructure on the Damping Properties of Stress-Strain Tool Systems in the Processing of Welded Structures from Dissimilar Steels. *Mater. Sci. Forum* **2021**, *1022*, 7–16. [[CrossRef](#)]
26. Popova, K.; Prošek, T. Corrosion Monitoring in Atmospheric Conditions: A Review. *Metals* **2022**, *12*, 171. [[CrossRef](#)]
27. Khaled, K.F.; Abdel-Rehim, S.S. Electrochemical investigation of corrosion and corrosion inhibition of iron in hydrochloric acid solutions. *Arab. J. Chem.* **2011**, *4*, 397–402. [[CrossRef](#)]
28. Fan, B.; Souriou, D.; Bosc, F.; Guilbert, D.; Kadkhodazadeh, S.; Ihamouten, A.; Fauchard, C.; Dérobert, X. Dielectric relaxation of iron corrosion products in limestone under saline environment. In Proceedings of the NSG2021 2nd Conference on Geophysics for Infrastructure Planning, Monitoring and BIM, Bordeaux, France, 9 August–2 September 2021; European Association of Geoscientists & Engineers: EAGE Publications BV: Houten, The Netherlands, 2021; pp. 1–5. [[CrossRef](#)]
29. Molodin, V.V.; Anufrieva, A.E.; Leonovich, S.N. An impact of concrete surfaces carbonization on their cohesion with newly-laid concrete. *Nauka Tekhnika Sci. Eng.* **2021**, *20*, 320–328. (In Russian)
30. Merzlyakov, M.Y.; Hernandez, J.R.R.; Zhapkhandayev, C.A. Development of cement slurries for oil and gas wells lining in aggressive environment. In *Youth Technical Sessions Proceedings*; Taylor and Francis Group Publishers: London, UK, 2019; pp. 387–393. [[CrossRef](#)]
31. Kreshkov, A.P. *Osnovy Analiticheskoy Khimii (The Fundamentals of Analytical Chemistry)*, 3rd ed.; Cengage Learning: Moscow, Russia, 1971; Volume 2, pp. 424–425. (In Russian)
32. Ivanov, I.I.; Dubovikov, O.A.; Grigor'Eva, L.V.; Kuzhaeva, A.A.; Zgonnik, P.V. Study of stability of constructional materials in melts containing lower titanium chlorides. *Russ. J. Appl. Chem.* **2011**, *84*, 1529–1531. [[CrossRef](#)]
33. Ivanov, I.I.; Dubovikov, O.A.; Grigor'Eva, L.V.; Kuzhaeva, A.A.; Zgonnik, P.V. Study of the corrosion stability of some materials in the titanium (II) and (III) chloride melts. *J. Min. Inst.* **2013**, *202*, 220–225.
34. Noubactep, C. Should the term 'metallic iron' appear in the title of a research paper. *Chemosphere* **2022**, *287 Pt 4*, 132–134. [[CrossRef](#)] [[PubMed](#)]
35. Faisal, M.; Roberts, K.P. Mechanistic modeling of erosion–corrosion for carbon steel. In *Trends in Oil and Gas Corrosion Research and Technologies*; El-Sherik, A.M., Ed.; Elsevier & Woodhead Publishing: Cambridge, UK, 2017; pp. 756–759. [[CrossRef](#)]
36. Hernandez, S.; Nassef, A.S. Erosion–corrosion. In *Trends in Oil and Gas Corrosion Research and Technologies*; El-Sherik, A.M., Ed.; Elsevier & Woodhead Publishing: Cambridge, UK, 2017; pp. 341–352. [[CrossRef](#)]
37. Qin, Y.; Li, Y.; Zhang, D.; Zhu, X. Stability and corrosion property of oil-infused hydrophobic silica nanoparticle coating. *Surf. Eng.* **2021**, *37*, 206–211. [[CrossRef](#)]
38. Smirnova, O.; Kazanskaya, L.; Koplík, J.; Tan, H.; Gu, X. Concrete Based on Clinker-Free Cement: Selecting the Functional Unit for Environmental Assessment. *Sustainability* **2021**, *13*, 135. [[CrossRef](#)]
39. Smirnova, O.M. Low-Clinker Cements with Low Water Demand. *J. Mater. Civ. Eng.* **2020**, *32*, 06020008. [[CrossRef](#)]
40. Yakovlev, G.; Polyanskikh, I.; Gordina, A.; Pudov, I.; Černý, V.; Gumenyuk, A.; Smirnova, O. Influence of Sulphate Attack on Properties of Modified Cement Composites. *Appl. Sci.* **2021**, *11*, 8509. [[CrossRef](#)]